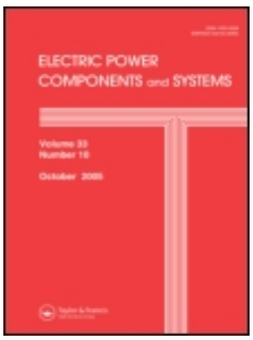

Taylor & Francis
Taylor & Francis Group

Electric Power Components and Systems

ISSN: 1532-5008 (Print) 1532-5016 (Online) Journal homepage: https://www.tandfonline.com/loi/uemp20

Investigation on Electromagnetic Transients of Distributed Generation Systems in the Microgrid

D. N. Gaonkar

To cite this article: D. N. Gaonkar (2010) Investigation on Electromagnetic Transients of Distributed Generation Systems in the Microgrid, Electric Power Components and Systems, 38:13, 1486-1497, DOI: 10.1080/15325008.2010.482090

To link to this article: https://doi.org/10.1080/15325008.2010.482090

Electric Power Components and Systems, 38:1486–1497, 2010

ISSN: 1532-5008 print/1532-5016 online
DOI: 10.1080/15325008.2010.482090

Taylor & Francis
Taylor & Francis Group

Investigation on Electromagnetic Transients of Distributed Generation Systems in the Microgrid

D. N. GAONKAR [1]

[1]Department of Electrical and Electronics Engineering, National Institute of Technology Karnataka, Surathkal, Mangalore (D.K.), Karnataka State, India

Abstract *The increasing interconnection of distributed generation sources of diverse technologies to low-voltage grids introduces considerable complexity in its operation and control. The concept of the microgrid is emerging as a solution to this and also to take full advantage of the potential offered by distributed generation. In this article, the performance of a typical microgrid with multiple distributed generation systems in grid-connected and autonomous modes of operation has been investigated through simulation. The developed model of the microgrid consists of a converter-interfaced microturbine generation system, a synchronous-generator-based distributed generation system, and a wind power generation system with an asynchronous generator. Investigation has been carried out to study the typical electromagnetic transients of a microgrid, due to preplanned and unplanned switching events. The performance of the bidirectional grid interface topology for a microturbine generation system in a microgrid is evaluated in this work. It has been observed from the simulation results that the motoring mode operation of the microturbine generation system during starting does not cause any disturbances in the microgrid. The study also indicates that the microgrid can maintain the desired power quality at the point of common coupling.*

Keywords distributed generation, microgrid, microturbine, converter interface, synchronous generator, wind power generation

1. Introduction

The operation and control of existing utility networks are becoming more and more complex due to the increased interconnection of a wide range of distributed generation (DG) systems. The present trend in technology toward smaller distributed generators, called microgeneration source, with a rating less than 500 kW, is further aggravating the situation. A brand new concept of microgrid is emerging as a potential solution [1, 2]. The microgrid is a systematic way of operating a section of network, comprising sufficient generating resources in the grid-connected or autonomous mode in an efficient, deliberate, and controlled way. The microgrid has a larger power capacity and more control flexibilities to fulfill system reliability and power quality requirements. This is in addition to all the inherited advantages of a single-DG system. The technical challenges

Received 1 June 2009; accepted 24 February 2010.
Address correspondence to Prof. D. N. Gaonkar, Department of Electrical and Electronics Engineering, National Institute of Technology Karnataka, Surathkal, Mangalore (D.K.), Karnataka State, 575 025, India. E-mail: dngaonkar@yahoo.co.in

associated with the operation and control of a wide range of DG systems, such as wind, photovoltaic, fuel cell, microturbine, and small conventional generators (diesel, gas turbine etc) connected in the microgrid, are immense [1, 2].

The development of technology that permits the operation of a microgrid has recently gained great momentum. A majority of microgeneration sources are interfaced with power electronic devices. Controlling these devices is a major concern in the microgrid operation [3, 4]. The operation and control of multiple-DG systems in a microgrid with a wide variation in their operating characteristics are quite challenging. Thus, the modeling and dynamic performance study of different combinations of DG sources in a microgrid becomes significant. Few studies have been reported to analyze the microgrid operation with multiple-DG sources [3–5]. One of the most important features of the microgrid is the islanded or autonomous operation. Some of the issues that are to be considered for the successful islanding operation of a microgrid are proper load sharing among DG units and their interaction. A voltage and frequency droop control scheme for a converter-based DG system for islanded operation was reported in [3]. The dynamics of asynchronous-generator-, synchronous-generator-, and converter-based DG systems in a microgrid was studied in [4]. The interaction between a conventional diesel generator and power-electronic-based DG system in a microgrid was studied in [5].

DG based on microturbine technology will likely become a dominant DG in the future power supply network [6]. These DG systems are quickly becoming an energy management solution that saves money, resources, and environment in one compact and scalable package—be it stationary or mobile, remote or interconnected with the utility grid. The combination of traditional wind power generation and microturbine-based DG can become a more viable solution in the DG market. Thus, the study of dynamic performance of these DG systems along with the conventional diesel generator in a microgrid is needed. In this article, the dynamic performance of a microgrid consisting of a microturbine generation (MTG) system, synchronous-generator-based DG (diesel generator), and wind generation system is analyzed. The model of the microgrid is developed in Matlab/Simulink (The MathWorks, Natick, Massachusetts, USA). An investigation has been carried out to study the typical electromagnetic transients of a microgrid, due to preplanned and unplanned switching events and the subsequent islanding process.

2. Microgrid System and Components

Figure 1 shows a single-line diagram of the system used to investigate the typical microgrid operational scenarios. The system is composed of a 480-volt distribution system connected to the utility main grid through a 13.8-kV radial line, which forms a microgrid. The microgrid includes three DG units. DG_1 is a 300-kW conventional diesel generator or a gas-turbine generator equipped with excitation and governor control systems. DG_2 represents the fixed-speed wind-turbine set with a rated capacity of 275 kVA, which is interfaced through an asynchronous generator. DG_3 is a 30-kW voltage source converter (VSC) interfaced to a single-shaft microturbine-based DG system. In the above, DG_1 and DG_2 are both non-dispatchable sources that do not quickly respond to power management of the system during transients and large disturbances.

The electrical part of DG_1 is represented by a sixth-order state-space model. The model takes into account the dynamic characteristics of the stator, field, and damper windings. Similarly, the electrical part of DG_2 is represented by a squirrel-cage induction

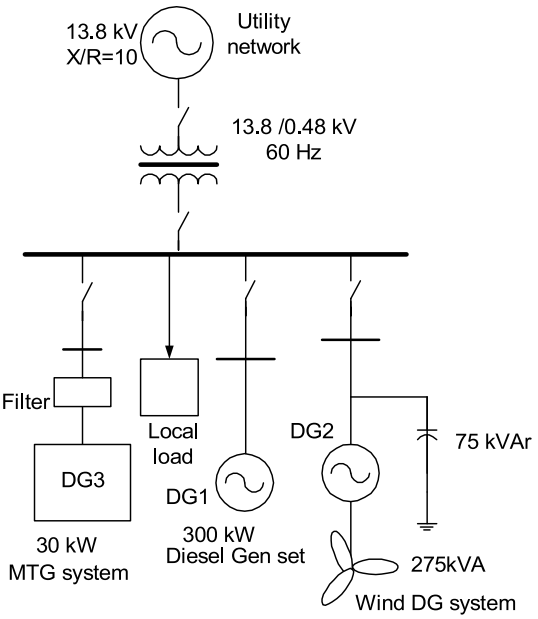

Figure 1. Study case for the microgrid.

generator connected to the utility grid. The mechanical part of DG_2, including the wind turbine and generator rotor, is represented by an equivalent of a two-mass dynamic system. The modeling of a wind power generation system using asynchronous generator (DG_2) and diesel generator systems (DG_1) were reported in [7].

DG_3 is interfaced to the grid using bidirectional VSC topology, which is implemented in Matlab/Simulink, as shown in Figure 2. This topology allows a bi-directional power flow between the converter and the grid, and hence, no separate starting arrangement is required. While starting, the permanent magnet synchronous machine (PMSM) acts as a motor and draws power from the grid to bring the turbine to a certain speed. In this, the line side converter acts as a controlled rectifier, and the machine side converter acts as an inverter and provides AC supply to the motor. This is also referred to as the motoring mode of operation of the PMSM. During the generating mode, the PMSM acts as a generator and power flows from the MTG system to the grid. A detailed modeling of individual components of the MTG system has been given in [8, 9].

In the grid-connected mode of operation, the DG units are expected to supply prespecified power to minimize the power import from the grid. Such requirements are system dependent and vary from system to system. In a grid-connected mode, each DG unit can be controlled to generate prespecified real and reactive power components or to generate prespecified real power and regulate its terminal voltage. The utility grid is expected to support the difference in real/reactive power requirements and maintain the frequency [3, 4]. In the autonomous mode of operation, the available power from the DG units must meet the total load demand of the microgrid. Otherwise, the system must undergo load shedding to match generation and load demand. In addition, fast and flexible real/reactive power control strategies are required to minimize the microgrid dynamics, such as islanding, and damp out system oscillations.

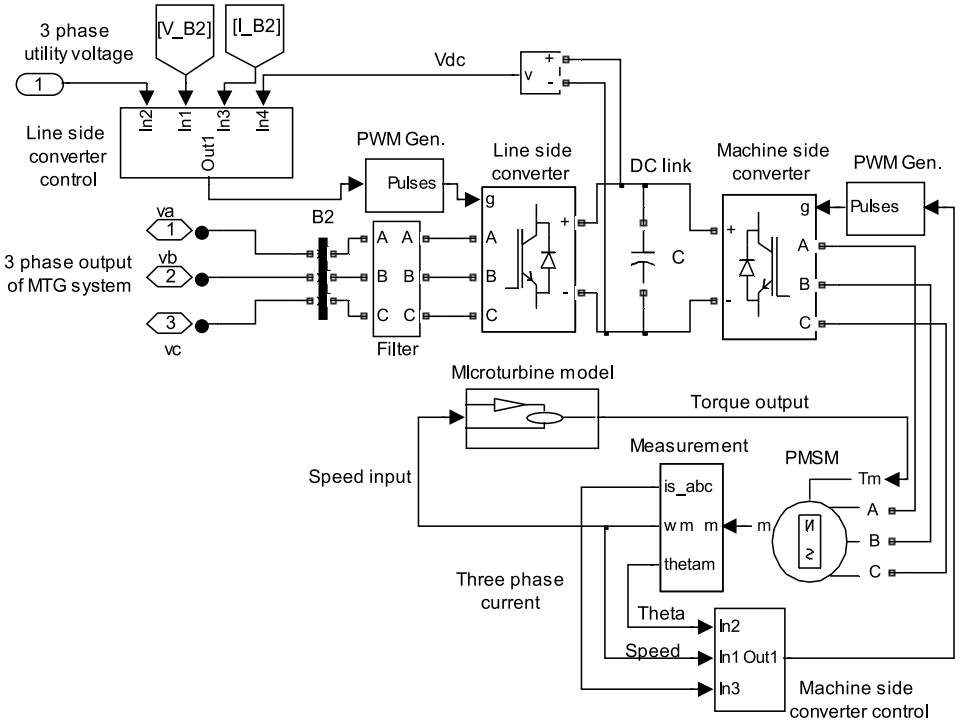

Figure 2. Simulink model of the MTG system.

3. Power Electronic Converter Control Strategies

Power electronic converters can be operated with different control strategies in a microgrid, depending upon the operation mode of the DG units. For the grid-connected mode of operation of a microgrid, converters can adopt either an active and reactive power control scheme (PQ control) [2] or control of active power and voltage (PV control [2, 3]. The former is the most commonly adopted control. In the PQ control mode, the converter controller regulates the active and reactive power injected to the grid. In this control, the converter acts as a current-controlled voltage source. This type of control can be easily implemented in the dq synchronous reference frame. This is achieved by regulating the active (i_d) and reactive component (i_q) of the injected current, with respect to reference values using proportional and integral controllers [8]. The design and Simulink implementation of the control scheme for grid-side and machine-side converters of the MTG system were given in [8, 9]. For the autonomous mode of operation of the microgrid, converters generally use voltage and frequency control with droop [3]. This control is necessary, as there is no voltage reference in the autonomous mode and also for proper load sharing in multi-DG environment of the microgrid.

4. Results and Discussion

The simulation model of the microgid structure, shown in Figure 1, with three DG sources is developed in Matlab/Simulink. The utility network is represented by a three-phase

Table 1
Simulation parameters for the model shown in Figure 2 [8]

Series RL filter	$L_f = 2.1$ mH, $R_f = 0.1\ \Omega$
PWM switching frequency	Grid side converter = 8 kHz Machine side converter = 20 kHz
DC-link capacitance	5000 μF
Proportional-integral controllers sampling time	100 μsec,
Machine side converter	$K_{p\omega} = 5$, $K_{pq} = 2$, $K_{pd} = 1.35$ $K_{i\omega} = 19.275$, $K_{iq} = 740$, $K_{id} = 499.99$
Grid side converter	$K_{pDC} = 0.015$, $K_{pq} = 2.5$, $K_{pd} = 2.5$, $K_{iDC} = 1$, $K_{iq} = 500$, $K_{id} = 500$
PMSM parameters	480 V, 30 kW, 1.6 KHz, 96,000 rpm, $R_s = 0.25\ \Omega$, $L_q = L_d = 0.0006875$ H
Microturbine parameters	Gain(K) = 25, $X = 0.4$, $Y = 0.05$, and $Z = 1$
Grid parameters	$R_s = 0.4\ \Omega$, $L_s = 2$ mH, 480 V, 60 Hz

balanced sinusoidal voltage source with internal impedance in series. The parameters of the microgrid and DG sources are given in Tables 1 and 2 [7, 8]. The wind turbine is assumed to operate with a constant wind speed of 10 m/s and a pitch angle (β) of zero. Several case studies are conducted to investigate the operation of the 480-V microgrid system in the grid-connected and islanding modes. Case studies are selected, so as to

Table 2
Simulation parameters for the synchronous generator, asynchronous machines, and microgrid [7]

Synchronous machine	
Machine rating	300 kVA, 480 V, 60 Hz, 4 poles
Inertia constant	$H = 2$ sec
Machine reactances in (p.u.)	$X_d = 3.23$, $X'_d = 0.21$, $X''_d = 0.15$, $X_q = 2.79$, $X''_q = 0.37$, $X_l = 0.09$
Stator resistances	$R_s = 0.017$ (p.u.)
Machine time constants in seconds	$T'_{do} = 1.7$, $T''_{do} = 0.008$, $T''_{qo} = 0.051266$
Asynchronous machine	
Machine ratings	275 kVA, 480 V, 60 Hz, 4 poles, squirrel-cage type
Inertia constant	$H = 2$ sec
Stator	Resistance (R_s) = 0.016 p.u. Inductance (L_s) = 0.06 p.u.
Rotor	Resistance (R_r) = 0.015 p.u. Inductance (L_r) = 0.06 p.u.
Mutual inductance	$L_m = 3.5$ p.u.
Resistive load	400 kW
Transformer rating	1.5 mVA, 13.8/0.48 kV

investigate the steady-state response to changes in the system operating point and the dynamic response when the system undergoes transient changes.

4.1. Grid-connected Mode

Initially, the microgrid operates in the grid-connected mode, where the load demand is supplied by DG_1, DG_2, and the main grid. Figure 3(a) shows the active and reactive power output of the diesel generator. The diesel generator supplies reactive power of 22 kVAr to the asynchronous generator as shown in Figure 3(a). Figure 3(b) shows the active and reactive power variations at the output terminals of the asynchronous generator. The speed of the asynchronous machine operating in the generator mode is slightly above the synchronous speed (1.011 p.u.), as shown in Figure 3(c). The wind turbine produces an output power of 206 KW for 10 m/s wind speed. Due to the losses in the asynchronous machine, the wind DG produces 200 kW, as shown in Figure 3(b). The total reactive power absorbed by the asynchronous generator is 97 kVAr, as shown in Figure 3(b). The three-phase capacitor bank connected across the terminal of asynchronous generator supplies 75 kVAr, and the balance of the power comes from diesel generator.

4.1.1. Starting of MTG System. A case study has been considered to investigate the starting performance of an MTG system on the operation of the microgrid. At $t = 2$ sec, the MTG system is started. During the start-up, the PMSM operates as a motor, and power flows from the grid to the MTG system. Figure 4(a) shows that the microturbine reaches the set value of speed (30,000 rpm) in 2.4 sec, and Figure 4(b) shows that it

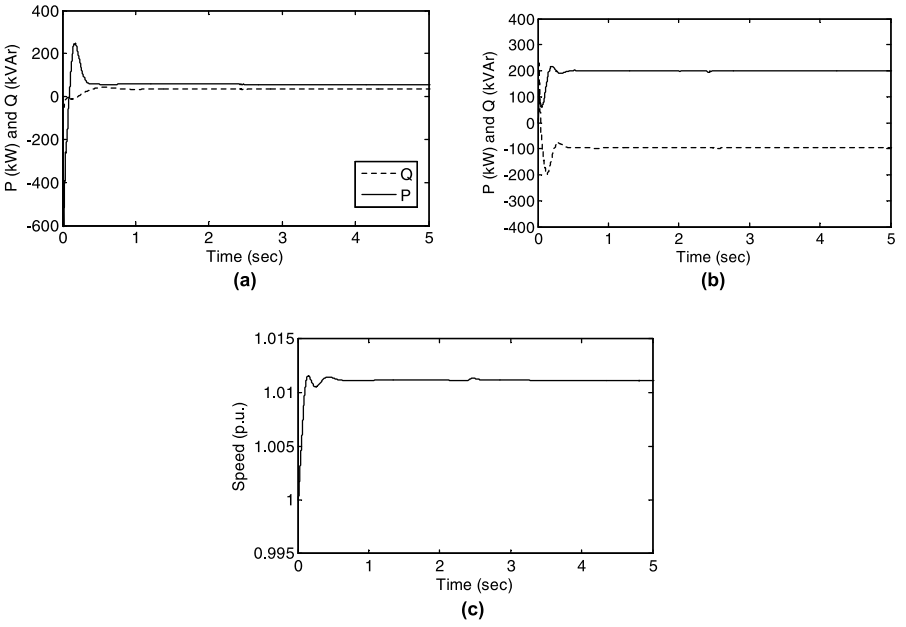

Figure 3. (a) Active and reactive power variations of synchronous generator, (b) active and reactive power variations of asynchronous generator, and (c) asynchronous generator speed.

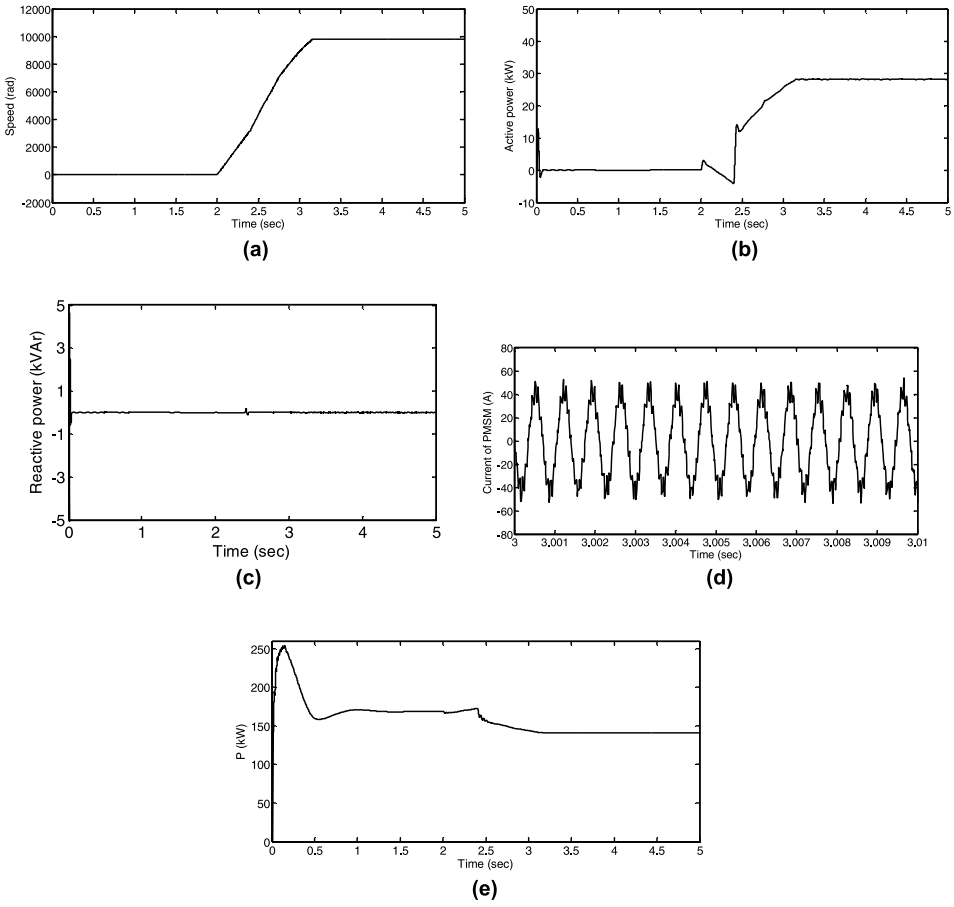

Figure 4. (a) Speed of the PMSM, (b) active power variations at the grid side of the MTG system, (c) reactive power at the grid side of MTG system, (d) detailed stator current variation of the PMSM, and (e) active power supplied by the grid.

absorbs power of 5.4 kW. To ensure this operating condition at a unity displacement factor, the precalculated reference speed and the direct current component i_d are set [8].

At $t = 2.4$ sec, the sign of the input torque of the PMSM is changed to operate in generating mode. The power starts flowing from the MTG system to the grid, as shown in Figure 4(b), and the output power reaches 28 kW in 3.2 sec. It can be observed that the change in operation mode of the PMSM in a simulation is instantaneous, but this may not be the same, practically because of the inertia of the machine. The reactive power variation at the grid side of an MTG system and the stator current variation of the MTG system are shown in Figures 4(c) and 4(d), respectively. The active power supplied by the grid during the simulation period is shown in Figure 4(e). The DC-link voltage variation across the capacitor is shown in Figure 5(a). It can be seen that the DC-link capacitor was charged to 760 V before starting the PMSM as a motor. It can also be seen from Figures 5(b) and 5(c) that the starting of an MTG system does not cause any voltage and frequency distortions. The total harmonic distortion (THD) at the load terminal is shown in Figure 5(d), and it is less than 5% [8].

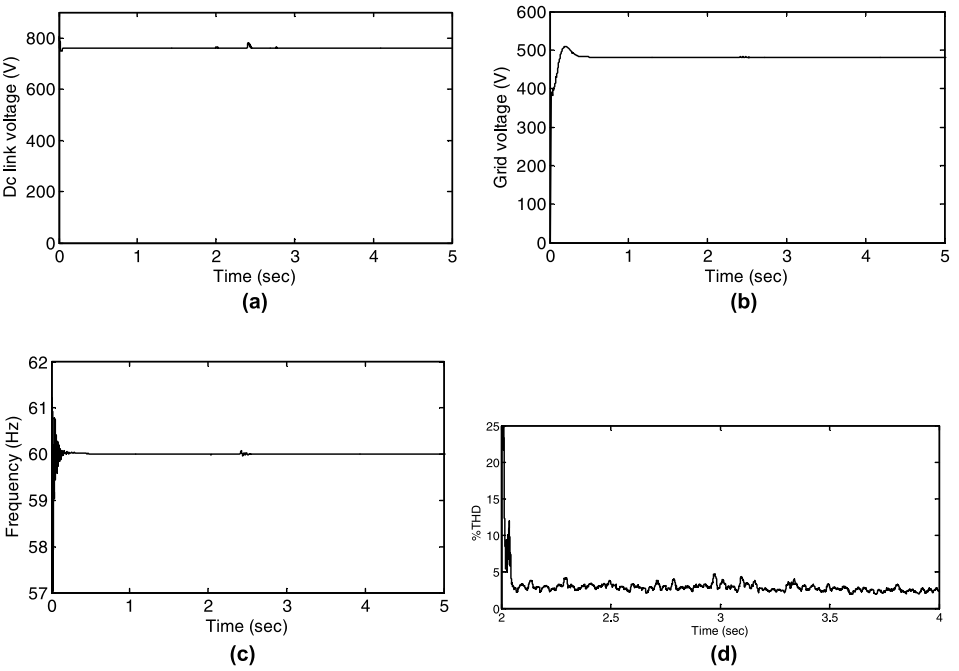

Figure 5. (a) DC-link voltage, (b) RMS voltage across the load terminals, (c) frequency variation of the microgrid, and (d) %THD variation at the point of common coupling.

4.2. Islanding Mode

Islanding of the microgrid can take place by unplanned events, such as faults in the medium-voltage (MV) network, or by planned actions, such as maintenance requirements. In the case of a preplanned microgrid formation, appropriate sharing of the microgrid load among the DG units and the main grid may be scheduled prior to islanding. Thus, the islanding process results in minimal transients, and the microgrid continues operation as an autonomous system. In the presence of unplanned events, such as faults, microgrid separation from the MV network must occur as fast as possible. However, the switching transient will have great impact on microgrid dynamics. The objective of this study is to investigate the transient behavior of the multiple DG units in the microgrid due to a preplanned islanding and unplanned islanding scenario.

4.2.1. Preplanned Islanding. The microgrid is disconnected from the utility by initiating a preplanned islanding command, which opens circuit breakers at $t = 3.6$ sec. Prior to this, the microgrid was operating in a grid-connected mode with DG_1 supplying 60 kW, DG_2 supplying 200 kW, and DG_3 supplying 28 kW, with the balance of the load requirement supplied by the grid. The MTG system is operating in a PQ-controlled mode. Figure 6 shows the dynamics of the microgrid during the islanding operation. The voltage variation during islanding conditions is shown in Figure 6(a). This is mainly due to the variation in the reactive power output of the DG systems.

The variation in the active and reactive power at the output terminals of the asynchronous generator are shown in Figure 6(b). It can be observed from Figure 6(b)

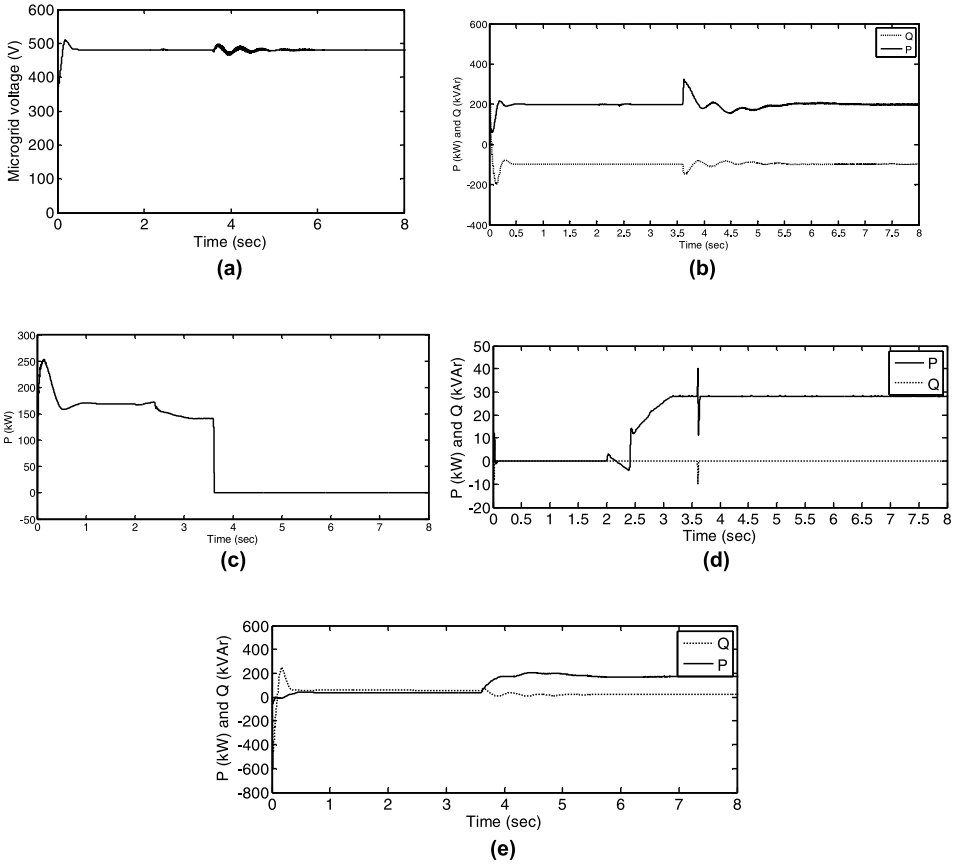

Figure 6. (a) RMS voltage across the load terminals, (b) active and reactive power variations of asynchronous generator, (c) active power supplied by the grid, (d) active and reactive power output of the MTG system, and (e) active and reactive power output of synchronous generator.

that a sudden change in active power output (P) and absorbed reactive power of the asynchronous generator (Q) takes place at the time of switching. The wind generation system is operated at a constant wind speed of 10 m/sec both during grid-connected and islanding modes. The active power output and reactive power absorbed by the asynchronous generator remains the same after the small transient time of 2 sec. During the autonomous mode of operation of the microgrid, power drawn from the grid is zero, as shown in Figure 6(c).

The active power output variation of the MTG system during the grid-connected and islanding mode is given in Figure 6(d). In this study, the MTG system is operated to supply 28 kW in both grid-connected and islanding operation modes. The reactive power reference for an MTG system is set at zero in order to obtain the unity power factor operation by injecting only active power to the grid. The variation in the active and reactive power output of a diesel generator is shown in Figure 6(e). During the autonomous mode, DG_2 and DG_3 together supply 228 kW, and the balance of the power requirement of the load is met by the diesel generator. From Figures 6(a), 6(b), and 6(c), it can be observed that during switching events, power electronic converter interfaced

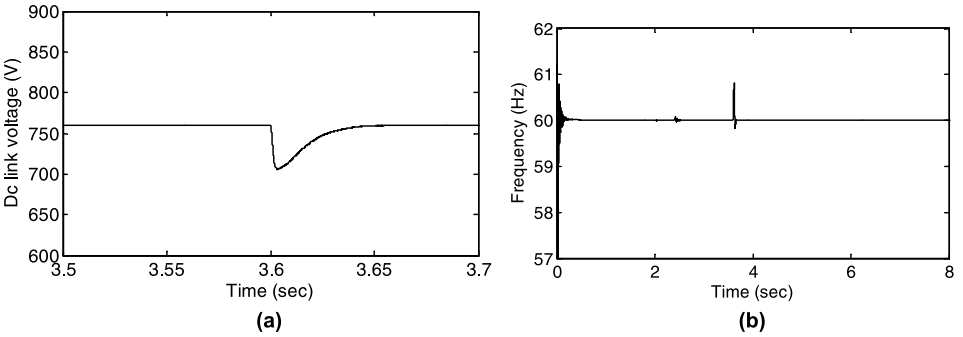

Figure 7. (a) DC-link voltage and (b) microgrid frequency.

DG systems act very fast to regulate their output compared to rotating-machine DG systems.

The DC-link voltage and its detailed variations are shown in Figure 7(a). A dip in the DC-link voltage can be observed at the time of switching from the grid-connected to the islanding mode. This is due to the sudden variation in the output power of the MTG system. The frequency of the microgrid is regulated to 60 Hz after the transient caused due to the switching event, as shown in Figure 7(b).

4.2.2. Unplanned Islanding. An unplanned islanding and microgrid formation is due to either system faults and its subsequent switching incidents or some other unexpected switching process. Prior to islanding, the operating conditions of the microgrid may vary; *e.g.*, the DG units can share the load in various manners, and the entire microgrid portion of the network may be delivering or importing power from the main grid. Furthermore, the disturbance can be initiated by any type of fault, and line tripping may be followed by single or even multiple reclosure actions. Thus, the severity of the transients experienced by the microgrid, subsequent to an unplanned islanding process, is highly dependent on (i) the preislanding operating conditions, (ii) the type and location of the fault that initiates the islanding process, (iii) the islanding detection time interval, (iv) the post-fault switching actions that are envisioned for the system, and (v) the type of DG units within the microgrid. An unplanned islanding of the microgrid system due to a three-phase-to-ground fault and its subsequent switching activities in the system is investigated in this section.

At $t = 3.5$ sec, a three-phase-to-ground fault is applied at the utility side. The three-phase-to-ground fault is cleared by the opening of circuit breaker, six cycles after the fault inceptions and a microgrid is formed due to the accidental islanding. Figure 8 shows the system transients during the unplanned islanding scenario. The prefault operating conditions of the system are the same as those of the preplanned islanding case. During the fault, bus voltages severely drop, as observed from Figure 8(a). Upon clearing the fault, the control action of the DG systems eventually return the voltages to their normal range. The variations in the active and reactive power of DG_1, DG_2, and DG_3 are shown in Figures 8(b), 8(c), and 8(d), respectively. DG_2 has no contribution to the fault current, while DG_3, because of employing a power electronic interface medium, has a limited contribution. However, DG_1 can inject reactive power up to ten times of its rating.

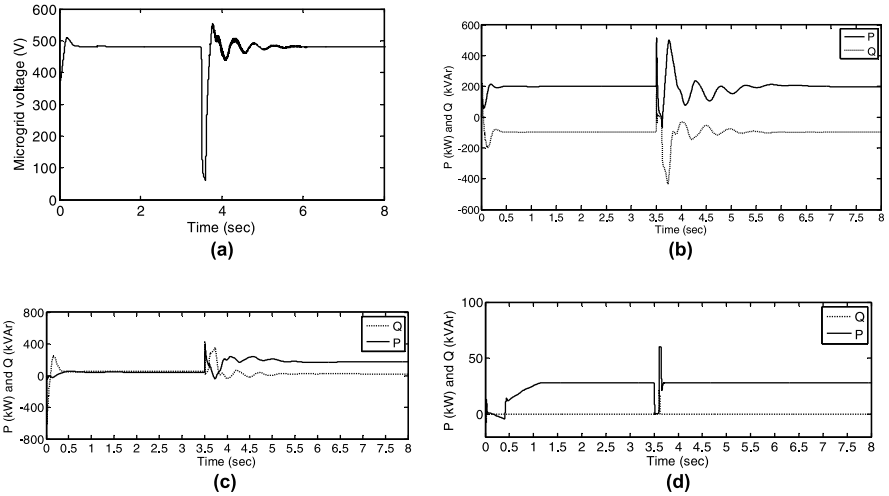

Figure 8. (a) RMS voltage across the load terminals, (b) active and reactive power variations of asynchronous generator, (c) active and reactive power output of synchronous generator, and (d) active and reactive power output of the MTG system.

5. Conclusions

This article presents an investigation on the dynamic performance of multiple-DG systems in a microgrid. The complete model of the microgrid has been developed in Matlab/Simulink. The structure of the microgrid considered in this study is typical, as it consists of both rotating-machine-based and power-electronic-interfaced DG systems. It is shown in this article that during the grid-connected mode of operation of the microgrid, starting of the MTG system does not cause any disturbance in the grid. It is observed from the simulation results that the power-electronic-interfaced MTG system can act faster in controlling disturbances compared to the rotating-machine-based DG systems. The study shows that the fast real and reactive power control provided by the power-electronic-interfaced DG systems can effectively manage the power fluctuation of the microgrid. The results indicate that the microgrid can maintain the desired power quality at the point of common coupling. The study indicates the need for some measures to ensure smooth transition of microgrid operation from grid-connected to islanding modes.

References

1. Lasseter, R. H., and Paigi, P., "Microgrid: A conceptual solution," *Proc. IEEE 35th Power Electronic Specialists Conference (PESC)*, Vol. 6, pp. 4285–4290, Aachen, Germany, 2004.
2. Lasseter, R. H., Akhil, A., Marnay, C., Stevens, J., Dagle, J., Guttromson, R., Meliopoulous, A. S., Yinger, R., and Eto, J., "White paper on integration of distributed energy resources: The CERTS microgrid concept," Berkeley Lab Report LBNL-50829, Berkeley, CA, 2002, available at: http://certs.lbl.gov/pdf/LBNL_50829.pdf
3. Lopes, J. A. P., Moreira, C. L., and Madureira, A. G., "Defining control strategies for microgrids islanded operation," *IEEE Trans. Power Syst.*, Vol. 21, No. 2. pp. 916–924, 2006.
4. Katiraei, F., and Iravani, M. R., "Transients of a microgrid system with multiple distributed energy resources," *Proceedings of the International Conference on Power Systems Transients (IPST'05)*, Montreal, Canada, 19–23 June 2005.

5. Zoka, Y., Sasaki, H., Yorino, N., Kawahara, K. C., and Liu, C. C., "An interaction problem of distributed generators installed in a microgrid," *Proceedings of the IEEE International Conference on Electric Utility Deregulation, Restructuring and Power Technologies*, pp. 795–799, Hong Kong, April 2004.
6. Scott, W. G., "Micro-turbine generators for distribution systems," *IEEE Industry Appl. Mag.*, Vol. 4, No. 3, pp. 57–62, 1998.
7. Gagnon, R., Saulnier, B., Sybille, G., and Giroux, P., "Modeling of a generic high-penetration no-storage wind-diesel system using Matlab/Power System Blockset," *Global Wind Power Conference*, Paris, France, April 2002.
8. Gaonkar, D. N., Pillai, G. N., and Patel, R. N., "Dynamic performance of microturbine generation system connected to grid," *J. Elect. Power Compon. Syst.*, Vol. 36, No. 10, pp. 1031–1047, 2008.
9. Gaonkar, D. N., Pillai, G. N., and Patel, R. N., "Seamless transfer of microturbine generation system operation between grid connected and islanding modes," *J. Elect. Power Compon. Syst.*, Vol. 37, No. 2, pp. 174–188, 2009.
10. Marwali, M. N., Jung, J. W., and Keyhani, A., "Control of distributed generation systems, Part 2: Load sharing control," *IEEE Trans. Power Electron.*, Vol. 19, No. 6, pp. 1551–1561, November 2004.